recycling

MDPI

Article

The Feasibility of Using Marble Cutting Waste in a Sustainable Building Clay Industry

Medhat S. El-Mahllawy *, Ayman M. Kandeel, Mahmoud L. Abdel Latif and Abdeen M. El Nagar

Raw Building Materials and Processing Technology Research Institute, Housing and Building National Research Center (HBRC), 87 El-Tahreer St., Dokki, Giza 12311, Egypt; amkandeel61@gmail.com (A.M.K.); ultramahmoudforever@gmail.com (M.L.A.L.); abdeenelnagar@yahoo.com (A.M.E.N.)

* Correspondence: medhatt225@yahoo.com

Received: 11 June 2018; Accepted: 29 August 2018; Published: 3 September 2018

Abstract: This study evaluates the feasibility of stabilizing clay bricks with marble cutting waste (MCW). This waste is currently discarded in huge quantities as sludge resulting from the sawing of marble blocks to slabs and the processes of disposing of grinding and polishing marble in landfills located around the marble processing factories in the Shaq El-Thoban industrial zone, Cairo governorate, Egypt, which causes negative impacts on the environment, health, and sustainable development. Experimental investigations were carried out to explore the effect of the addition of MCW in different clay–base mixes using varying percentages of up to 20% at the expense of the hydrated lime. Cement, hydrated lime, and MCW are the three types of solidification agents used, and clay and sand were also added in the formulations of the unfired clay brick specimens. Laboratory cylindrical stabilized and compressed specimens were made; then, they were cured in a humidity chamber for two weeks and four weeks. Afterwards, they were air dried, tested, and evaluated according to the Egyptian code for the building by the stabilized and compressed earth soil (ECBS, 2016). To enhance the durability of the cured specimens, transparent silicon-based paint was used. The results demonstrated that the optimum content of marble sludge waste (MCW) was 15% when used as replacement for hydrated lime in the production of stabilized clay brick. For all of the samples, the use of silicon-based paint was found to improve the strength and water resistance of the stabilized clay bricks. The use of local waste materials as a substitute for a hydrated lime binder reduces both the cost and environmental impact associated with block production.

Keywords: marble cutting waste; stabilized clay bricks; hydrated lime; Shaq El-Thoban industrial zone

1. Introduction

In Egypt, clay brick has long been the most common construction material used for historical and traditional buildings. Conventional bricks are produced from clay using a high firing temperature or from ordinary Portland cement (OPC) with aggregates. The high temperature used or the clay bricks and cement processing industries consume a significant amount of energy, and release a large quantity of greenhouse gases to the atmosphere, leading to environmental and economical problems. In the clay brick industry, about 0.41 kg of carbon dioxide is released per brick [1]. In the cement industry, the production of OPC is responsible for about 7% of all CO_2 generated worldwide [2]. So, for environmental protection and sustainable development, many researchers have studied the utilization of waste materials and industrial by-products to make eco-friendly building bricks using different methods, materials, and stabilizers [3–10].

Several positive reactions occur when lime is added to clay in the presence of water; cation exchange, flocculation–agglomeration, carbonation, and pozzolanic reaction [11]. In contrast, two deleterious chemical reactions probably occur in the lime-treated soil [12]. The first is lime carbonation, and the second is the reaction with the sulfate salt existing in the soil. Calcite crystals are formed due to the carbonation process, which is considered a cementing material, but its formation should be controlled. This is due to three main reasons: it has a weak bonding force, calcium carbonate is a soluble salt when exposed to air for a long time period, and the carbonation process consumes calcium ions, which have a negative affect on the role of lime in the pozzolanic reaction progress. The most common global usage of marble sludge waste in the construction field is for cement, concrete production and composites, the corrosion resistance of steel rebars, fired brick, and in the stoneware industry [13–16]. Also, a study has been published [17] on the characterization and recycling potentiality of Egyptian marble sludge and its compatibility for use in different industrial applications. The study suggested using the sludge in the following applications, taking into consideration its chemical composition, whiteness, humidity, and grain size: the manufacture of cement, water paints, fertilizers, animal food, iron and steel, paper, plastic, ceramic, bituminous mixes, and marble resin products. Almost no publications were found to investigate the use of MCW as an additive for the production of non-burnt clay brick.

In Africa, compressed stabilized earth bricks are widely used in construction, as they are the most efficient way of building and have many advantages [18]. Sustainability involves the use of waste materials and by-products produced from other industrial activities in green and useful applications. In this research, during the cutting stage of the Egyptian marble processing industry, the marble cutting waste (MCW) is generated in the form of fine particles as aqueous sludge. In Egypt, the main area where most of the marble factories and manufacturing plants are found are located in the Shaq El-Thoban industrial zone, Cairo governorate. It contains about 400 factories and 3000 manufacturing workshops [19]. These manufacturing places produce nearly 3–4 million tons of marble and granite products that generate about 0.8–1.0 million tons of marble and granite waste per year [17]. The MCW that is used is the result of sawing marble blocks to slabs and the processes of grinding and polishing of marble as a liquid slurry waste. It is discarded daily in large quantities to nearby pits or vacant spaces near the marble processing industries, although notified areas have been marked for dumping. This leads to an increase in environmental risks as dust pollution spreads along a large area. In the summer season, the dust dries up, floats in the air, and flies, generating a huge amount of fine wastes, which certainly creates severe negative ecological impacts for flora, fauna, human health, and sustainable development. The accumulated waste may also contaminate surface and underground water reserves, and lead to land degradation. So, the main objective of this study is to evaluate the feasibility of stabilizing clay-based bricks with the Egyptian marble cutting waste (MCW) for economical, environmental, and health concerns.

2. Experimental Procedures

2.1. Materials

Five different materials were used in this study: Kafr Homied clay (KHC), sand, ordinary Portland cement (OPC), marble cutting waste (MCW) and hydrated lime (HL). The stabilizers were HL and OPC. The used clay and sand samples were collected from the clay and sand quarries located beside Kafr Homied village, which is 50 km south of Cairo in Giza governorate, Egypt. In the field, the clay that is used is grayish green in color, massive, damped, and has some gypsum lamina of different directions and iron oxide spots included within the claystone deposits of the late Eocene age [20]. The Portland cement used was of CEM (I) 42.5 type, and locally manufactured and supplied by the Suez Cement Company, Egypt. The used hydrated lime was purchased from the most common type in the Egyptian market. The marble waste used in this investigation was delivered as air-dried powder residual from the marble landfill at Shaq El-Thoban area, east of Auto Strad Rd., Cairo governorate (Figure 1). It is

the largest marble and granite industrial cluster in Egypt, and the fourth world-industrial zone. Also, a silicon-based paint was used in this study for the specimen treatment to increase their durability. It was obtained from the CMB (chemicals for modern buildings) group, exterior paint products, Egypt.

Figure 1. Photographs showing types of the cutting processes (**a**,**b**), marble cutting sludge (**c**), marble polishing process (**d**), Cairo, Egypt.

2.2. Methods

Selective samples from the materials used and laboratory-made unfired cylindrical clay specimens were analyzed by powder X-ray diffraction (XRD) for mineralogical characterization. The used XRD apparatus was a X'Pert PRO PW3040/60 (PANalytical) diffractometer equipped with a monochromatic Cu–Kα radiation source. The test was run at 40 kV and 30 mA. The acquired data was identified using X'Pert high score software works with a PDF-2 database. The chemical composition (major oxides) of the raw materials used was determined by X-ray fluorescence (XRF). The used XRF was an Axios sequential spectrometer manufactured by PANalytical, Netherlands. Also, a traditional manual method prescribed in the American Society of Testing and Materials (ASTM) for the determination of loss on ignition (LOI) [21] was followed. The particle size distribution of the used materials was determined using a laser diffraction analyzer (manufactured by Horiba, LA-950, France). Furthermore, the pH value was measured at 20 °C by an electronic pH meter (Jenway 3510, UK) following the ASTM test method [22]. The formed phases in the cured specimens were identified using a Jasco-6100 Fourier transformed infrared spectrometer (FTIR; Varian model, Excalibur FTS 3000MX, Paolo Alto, CA, USA). The tested samples were prepared using the KBr pressed disc technique. The analysis was done between 400–4000 cm^{-1}.

2.3. Mix Composition and Specimen Preparation

In order to investigate the effect of the MCW used, five mixes, namely R (control mix), R 1, R 2, R 3, and R 4 were designed for the study, as given in Table 1. The MCW was added at the expense of the HL content. The Portland cement was added in a small percentage for economical and environmental concerns, and to accelerate the initial bonding between the mix components. The sand as a non-plastic

material was used to make the final product durable [23] and reduce the effect of shrinkage of clay, which may occur as well, in order to accelerate the formation of hydration products [24]. All of the used materials were passed through a 300 micron diameter sieve before the experimental work.

Table 1. Composition, proportion, and pH of the studied mixes. HL: hydrated lime, MCW: marble cutting waste, OPC: ordinary Portland cement.

Mix Code	Mix Ingredient, %					pH
	Clay	Sand	HL	MCW	OPC	
R	75	25	0	0	0	6.7
R 1	50	25	20	0	5	12.8
R 2	50	25	10	10	5	12.5
R 3	50	25	5	15	5	12.4
R 4	50	25	0	20	5	11.5

The mixing process of the mixes was started by thoroughly mixing the ingredients of each mix by manual shaking and overturning the plastic bag for at least 2 min. The water was added gradually (approx. ~16% of the total mix wt.) to the prepared mix in a laboratory mixer, and then mixed for at least 3 min to obtain a homogenous mix. Then, the mix was placed in a cylindrical mold of 25-mm diameter and 50-mm height, and compressed using a static hydraulic compression machine under 10.0 MPa of pressure. The specimens mixture was then demolded ~10 s after completion of the compaction; then, it was labeled and stored in a controlled humidity chamber at 40 °C ± 2 and 80% ± 2 relative humidity (RH) until the testing times of 14 days and 28 days. Five sets of compacted specimens were laboratory-made. The cured specimens were air dried for three days before starting the physico-mechanical tests. Generally, dynamic compaction can reduce the optimum water content from 12% to 10% with about a 50% increase in the compressive strength and an optimum water content range between 10–13% for static compaction [25].

2.4. Testing Procedures

At the end of the curing periods (14 days and 28 days), a series of tests were carried out in order to determine the primary engineering properties for the air-dried specimens in terms of water absorption, bulk density, soaking test, and compressive strength. To simulate the manufacturing process, before every test, the specimens were naturally dried for three days at lab ambient conditions (air-dried specimen). The tests were carried out according to the following formulations: A water absorption test was measured using the relation (Ms-Md)/(Md), where Ms is the mass of the saturated-dry specimen (g) after 24-h of water soaking, and Md is the mass of the air-dried specimen (g). The bulk density of the specimens was determined by dividing the mass of the air-died specimen (g) by the volume of the cylindrical specimen (cm^3). The compressive strength test was calculated by dividing the maximum load to failure (kg) by the area of the bearing surface (cm^2) of a specimen. To evaluate the durability of the specimens against water, the air-dried specimens of different mixes with different curing periods were soaked completely in tap water for 24 h, and the result was visually assessed. Also, to enhance the specimens' durability, the 14-day air-dried specimens were surface treated by a silicon-based paint, and the water-soaking test was carried out again and evaluated. The elapsed time between the painting and testing of the painted specimens was three days at lab ambient conditions. Also, all of the air-dried and treated specimens were tested for water absorption, bulk density, soaking, and compressive strength. The average of three test results was recorded, if available. The test results were evaluated in accordance with the Egyptian code for building by stabilized soil [26].

3. Results and Discussion

3.1. Characteristics of the Raw Materials

The chemical composition, loss on ignition (LOI), and pH of the used materials are given in Table 2. The used quicklime (HL) is not a fatty lime (CaO < 85%) according to the Egyptian standard specification [27]. The XRD patterns of the used clay, sand, and OPC have been illustrated before [28]. The chemical composition of the KHC shows about 3% of SO_3, expecting the presence of sulfate-based mineral (gypsum), as confirmed by the XRD analysis. The MCW consists mainly of CaO content with minor percentages of the other oxides and traces/minor contents of chloride ion, alkalis, and iron oxide. The pH of the MCW is slightly alkaline. Figure 2 shows the XRD pattern of the used MCW. The pattern confirms the results of the chemical analysis, where the waste is composed mainly of calcite mineral ($CaCO_3$), and traces of quartz (SiO_2) mineral are also detected.

Table 2. Chemical compositions in terms of oxide content (wt.%), loss on ignition (LOI), and pH of the raw used materials.

Oxide Content %	Hydrated Lime (HL)	Ordinary Portland Cement (OPC)	Clay	Sand	Marble Cutting Waste (MCW)
SiO_2	1.69	20.59	49.95	93.88	0.52
Al_2O_3	1.11	4.02	22.51	3.86	0.12
Fe_2O_3	0.24	3.31	6.87	0.68	0.18
CaO	70.52	62.71	1.64	0.65	56.35
MgO	0.75	1.95	1.22	0.37	0.35
Na_2O	0.01	0.47	3.11	0.21	0.05
K_2O	0.05	0.18	0.92	0.09	0.04
SO_3	0.14	2.95	3.12	0.02	0.01
L.O.I	25.69	3.81	10.28	0.23	42.38
pH	12.82	13.52	6.72	7.11	8.13
Cl^-	Nil	Nil	0.86	Nil	0.01

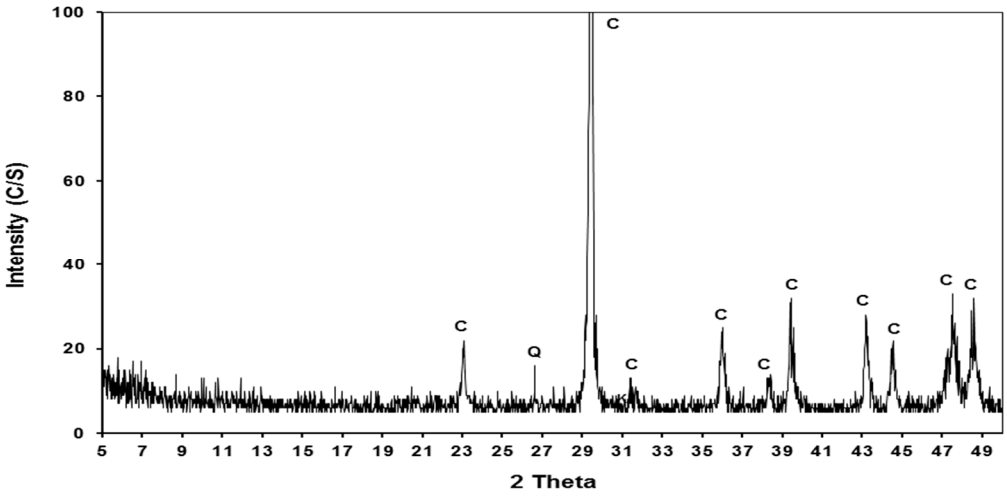

Figure 2. X-ray diffraction (XRD) pattern of the MCW used (C: Calcite, Q: Quartz).

Figure 3 presents the particle size distribution analysis of the used MCW. The pattern shows bimodal peaks representing the biggest quantitative percentages that are found at 5.0% and 4.5%. Ninety percent of the particle sizes are under 21.4 μm, and the biggest particle size is 262.3 μm. Also, the mean particle size is 13.1 μm. The results illustrate that the tested MCW particles are within the medium silt size class.

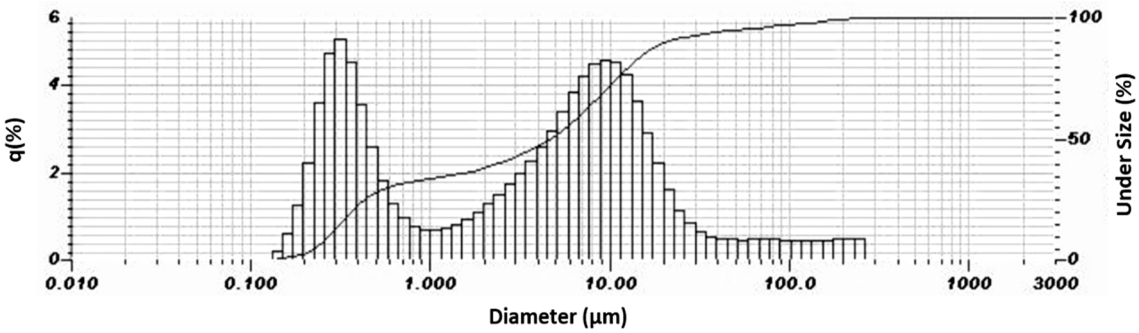

Figure 3. Particle size analysis of the used MCW.

3.2. Mineralogy of the Cured Specimens of Different Mixes

Figures 4 and 5 represent the XRD patterns of the clay-based specimens of different mixes cured for two weeks and four weeks, respectively. As shown in Figures 4 and 5, the identified phases are montmorillonite, kaolinite, albite, quartz, calcite, gypsum, ettringite, and calcium silicate hydrate (CSH). The main crystalline phases are quartz and calcite of different peak intensities. It was observed that as the MCW increases to less than 20% (mixes R1–R3), in the presence of HL, the peaks of clay minerals decreased, and finally disappeared, as shown in mix R3. The lack of clay minerals suggests their destruction and the formation of cementing and poorly crystalline gels. The reaction between the released soluble compounds and the calcium ions from the lime hydration creates cementitious materials such as a C–S–H gel and C–A–H [29]. These pozzolanic reactions are generally time-dependent, and require a long time. This is because such reactions are functions of temperature, calcium quantity, pH value, and the quantity of the soluble compounds. It is worth mentioning that the quartz peak intensity decreased with the increase of MCW content, as well as the procession of curing days (R1 to R4). Also, it was found that with the increase of the MCW addition, the calcite became well crystallized, which was obviously visible in the XRD pattern of mix R 4 (20% MCW and 0% HL). Calcite is expected to show a weak cementing bond between the particles. Furthermore, it is believed that the ettringite that is formed may be due to the chemical reaction between calcium ions (MCW) and the aluminum solubilized from the clay in the presence of a soluble sulfate (gypsum) and humidity for a long period of time. This formation is promoted in the absence of HL, as shown in mix R4, which has 0% HL.

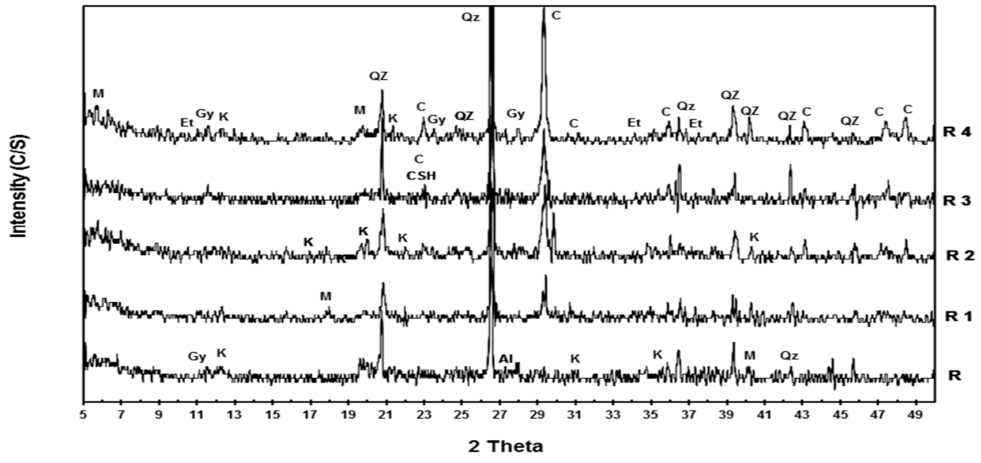

Figure 4. XRD patterns of the specimens of different mixes that had been cured for two weeks (M: Montmorillonite, Et: Ettringite, Gy: Gypsum, K: Kaolinite, Qz: Quartz, C: Calcite, CSH: Calcium silicate hydrate, Al: Albite).

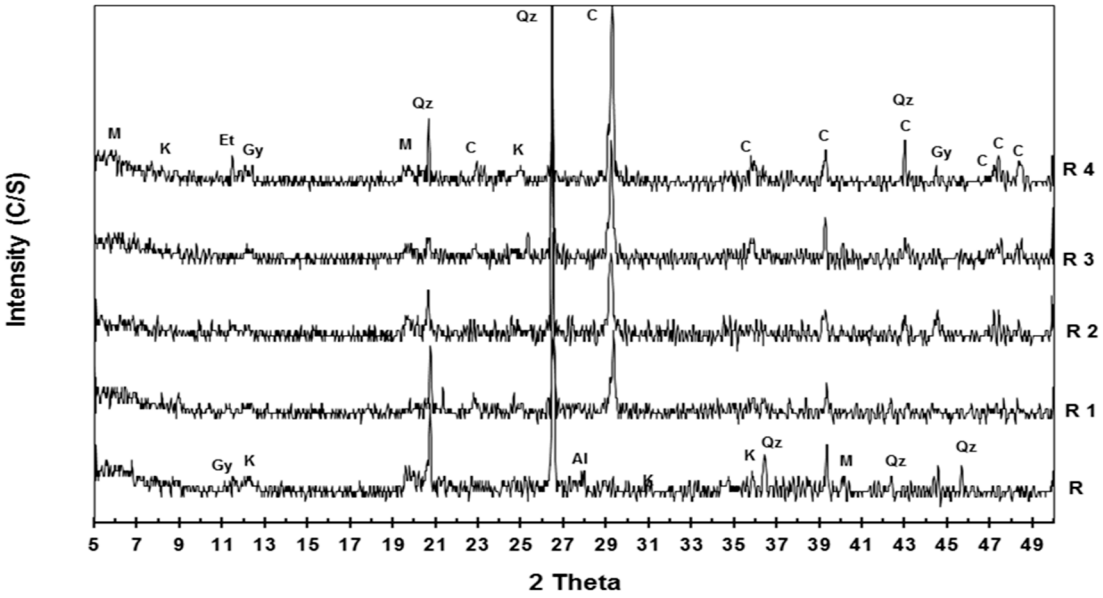

Figure 5. XRD patterns of the specimens of different mixes that had been cured for four weeks.

The excessive amount of calcite that appeared in the specimens of mix R4 limited the formation of the cementing hydrated compounds. Also, it was observed with the absence of the main stabilizer (HL) in mix R4, the ettringite and gypsum phases appeared. The ettringite formation may lead to an increase in the soil volume, water absorption, the reduction of effective cohesion, and soil strength loss [30].

The high pH value creates favorable conditions for local dissolution, which would likely release alumina and silica within the specimen body. Furthermore, the silica and alumina that exist in the clay minerals becomes soluble and free from the clay body when the pH exceeds 12 [12]. So, the specimens of mix R4 have no pozzolanic reaction, because the pH is 11.5. This is supported by the re-presence of clay minerals of kaolinite and montmorillonite. The significant change in the XRD patterns of the studied mixes that were cured for two and four weeks was found for the quartz peaks that had less intensity in the four weeks of curing. Moreover, the low crystallinity of the formed cementing phases (CSH), especially in the early stages of curing, has been supported before [31].

3.3. Physico-Mechanical Properties of the Cured Specimens

Figure 6 shows the results of the water absorption, bulk density, and dry/wet compressive strength of the specimens of different mixes cured for two and four weeks. Figure 7 represents the effect of treatment by the used silicon-based paint on the properties of the specimens of different mixes that had been cured for two weeks. Table 3 records the soaking test results of the specimens that had been cured for two and four weeks, and the results of the two-week cured specimens after the treatment.

The results of Figure 6 show that the water absorption decreased as the curing period increased. Also, the water absorption test cannot be determined for the specimens of mix R (without stabilizers) due to their collapsible behavior in water. It was noticed that the values of the absorbed water decreased as the MCW dosage increased, giving evidence that the MCW plays a significant role in the impermeability of the tested specimens in the presence of HL. It reached the best value (10.1%) in the R3 specimens (15% MCW + 5%HL) that were cured for four weeks. This is probably due to the pozzolanic reaction development, as obviously detected in the XRD patterns, which leads to the formation and accumulation of cement phases that closes some of the open pores, and decreases their affinity to absorb water. All of the specimens of mixes R1–R3 that were cured for two and four weeks achieved the ECBS requirements (class A: 8–10, class B: 10–12, and class C: 12–15%).

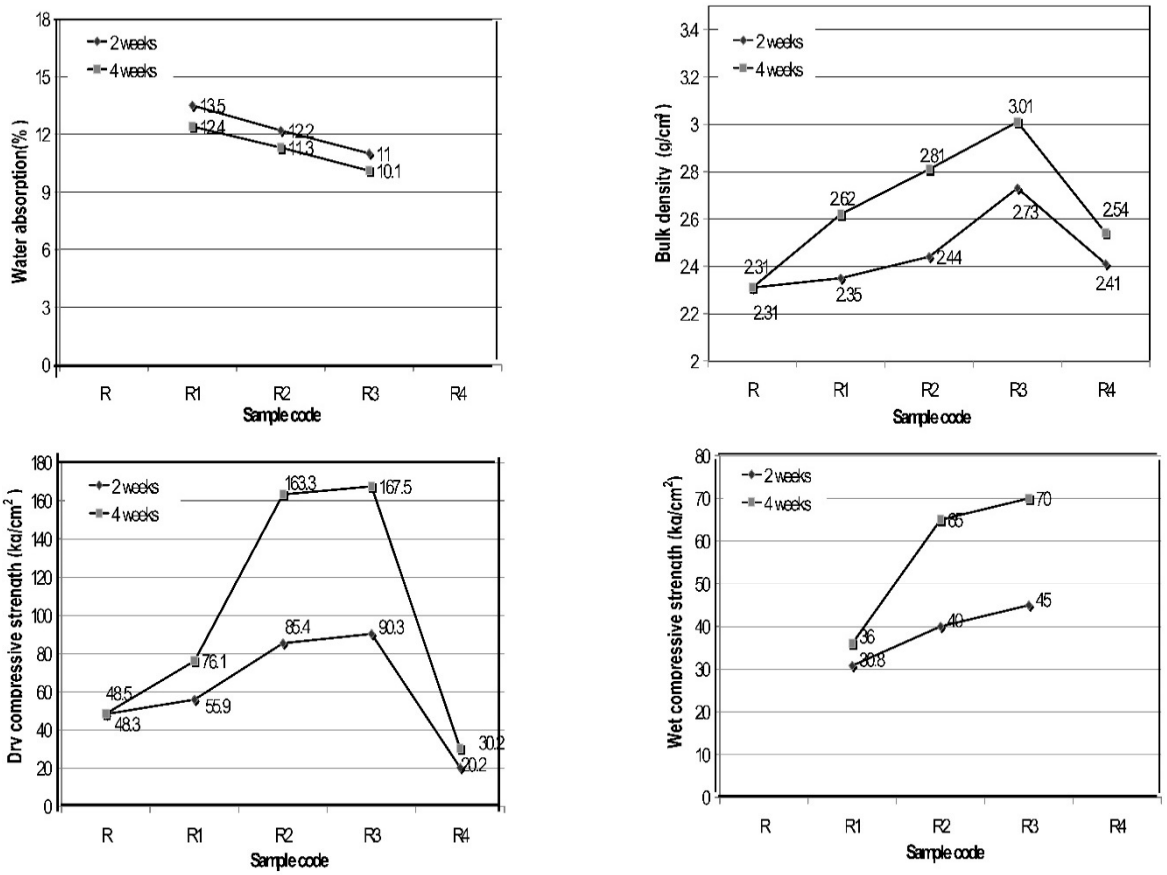

Figure 6. Water absorption, bulk density, and dry and wet compressive strengths of the specimens of different mixes cured for two and four weeks.

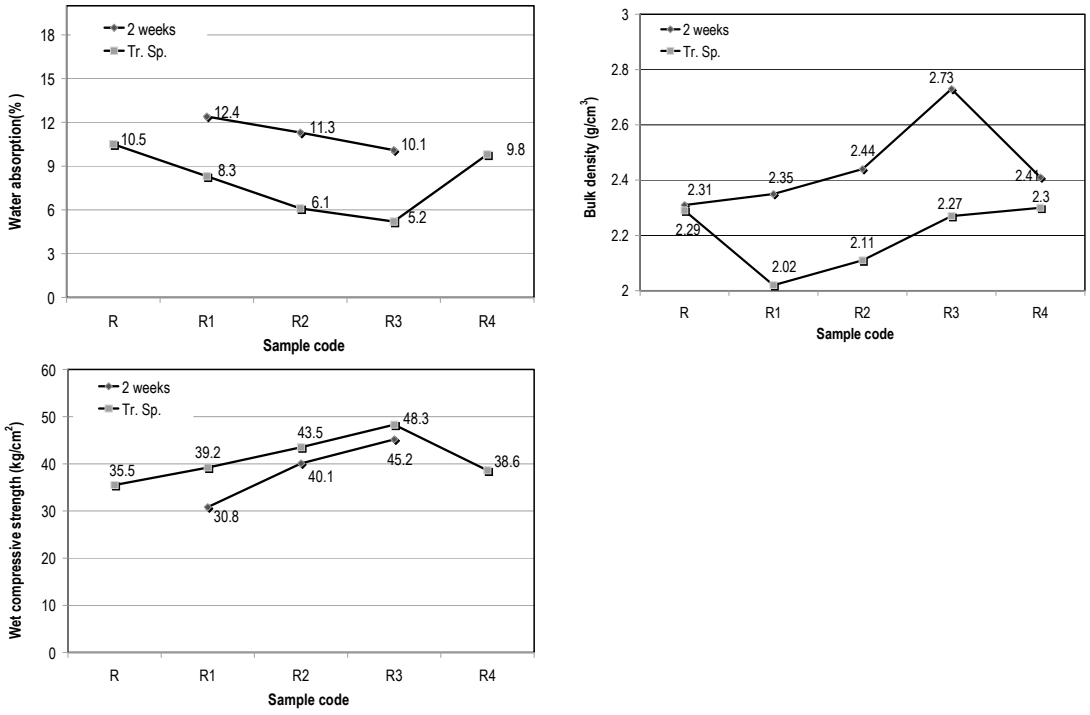

Figure 7. Comparison properties between the treated specimens (Tr. Sp.) and specimens cured for two weeks.

Table 3. Result of the water soaking test of the cured specimens of different mixes before and after treatment.

Specimens of the Mix	Status of the Specimens Cured for		
	2 Weeks		4 Weeks
	Before	After	
R	C	PF	C
R1	PF	ND	PF
R2	ND	ND	ND
R3	ND	ND	ND
R4	C	ND	C

ND: No damage, PF: Partial failure (after a while), C: Complete failure.

In terms of bulk density (Figure 6) of the clay-based specimens, it increased with the curing period, as well as the MCW addition until mix R3. The specimens of mix R4 showed the lowest density compared to the other mixes. The bulk density increase is indicative of the pozzolanic reaction progressing, phases formation, and vice versa. The highest value was achieved by the specimens of mix R3, which were cured for four weeks. In other words, as the MCW content increased at the expense of the HL, the bulk density increased, giving evidence of densification.

Figure 6 points to the compressive strength increasing with the prolongation of the curing period, and MCW content increasing until mix R3. The dry compressive strength values are remarkably higher than those of the wet results. The wet compressive strength of the specimens of mixes R and R4 at all of the curing periods could not be determined due to their collapsing in water. The soluble lime ions have a slow setting time, and gain their strength over time. In terms of comparing the strength development, the MCW is more effective in incorporating a low content of the HL. However, when the MCW dosage was too high (20%) and without the HL, the strength that was gained was too low. The highest value (167.5 kg/cm^2) was achieved by the specimens of mix R3 that were cured for 4 weeks. All of the cured specimens of mixes R1–R3 achieved the ECBS requirements of the dry and wet compressive strengths (dry compressive strength, class A: 50–70, class B: 40–60, and class C: 30–50%; and wet compressive strength; class A: 30–40, class B: 20–30, and class C: 15–20 kg/cm^2). The MCW may also act as a water-repellent material.

In order to enhance the specimen's properties of different mixes in terms of water absorption, wet compressive strength, and resistivity to the effect of water, the specimens that were cured for two weeks were treated by a silicon-based transparent construction paint, and had the lowest property values. The material was painted on the external surfaces of the specimens; thus, when dry, it gives an invisible waterproof protection that repels rain drops, which then slide over the surface and wash away dust and other pollution.

A comparative analysis between the obtained results was established and is represented graphically in Figure 7 and given in Table 3. As shown in Figure 7, all of the studied properties are clearly enhanced. The water absorption decreased after the treatment. This means that the treatment is effective, and it coats the external surfaces. Furthermore, as the used liquid has low viscosity, eases to penetrate inside the specimens, and has a low density (1.0 kg/L), the specimen's bulk density decreased, and their durability increased as compared with the specimens without treatment that were cured for two weeks.

The results given in Table 3 indicate the improvement of the specimen's resistivity to water collapsibility for the specimens of mixes R, R1, and R4. The results emphasize the importance of the use of surface protection paints in a wet environment, but it may need to evaluate the durability against water erosion using the spray test method.

The test results indicate that the good property values for the tested specimens may be attributed to the flocculation process and the calcite formation due to the carbonation of the added HL (R1–R3).

Furthermore, the higher strength development of the stabilized clay–HL–MCW–OPC (R1-R3) system with curing periods may be attributed to the gradual continued formation of C–S–H gel within the pore structure, without necessarily developing a crystalline structure, as recorded in the publication [32]. Also, the excessive amount of the MCW (R4) that has inert calcite negatively affected the stabilization process. Moreover, the HL plays an important role in the stabilization process of the clay-based mixes.

3.4. Results of the FTIR Analysis of the Cured Specimens of Different Mixes

Figures 8 and 9 depict the FTIR spectra of the specimens of different mixes that were cured for two weeks and four weeks, respectively. The matching in the band locations is obvious, and the difference is only in the band intensity. The detected bands were interpreted according to many authors [32–35]. The characteristic vibration bands at 3700 cm^{-1} and 3625 cm^{-1} are attributed to the O–H stretching of kaolinite and montmorillonite, respectively. These band intensities decreased as the MCW content and curing periods increased. This provides evidence to the diminishing of the clay content (clay dissolution) and formation of new phases. The bands at 3400 cm^{-1} and 1625 cm^{-1} can be attributed to the stretching vibration of the O–H group in the H_2O that was adsorbed on the specimens. The group of bands that were found in Figure 9 at 800 cm^{-1}, 1450 cm^{-1} (large and symmetric peaks) and between 2500–1800 cm^{-1} can be assigned to the vibration corresponding to the CO_3^{2-} group of calcite. These bands nearly increased as HL content increased and MCW decreased. All of the specimens had complex intensive silicate bands, Si–O, Si–O–Al (octahedral Al), Si–O–Si stretching and bending, as well as OH (Al_2OH) bending bands in the region of 1125–400 cm^{-1}. Generally, it is difficult to interpret this region by studying FTIR spectra only, since many forms of silicates give rise to several peaks, causing lots of overlaps. The band that appears as a shoulder at 1125 cm^{-1} and 675 cm^{-1} may be related to the unsolubilized silica. These bands decreased as the MCW increased and as curing period progressed. Also, a significant change was observed in the broadness in the band at 1000 cm^{-1}, which gradually increased with the increase of MCW content at the expense of decreasing the band intensity of the unsolubilized silica. This is parallel to the XRD results. This is supported by the growth of the increasable band in mix R3 at 3400 cm^{-1}, which may be indicative of the formation of pozzolanic reaction products. On the contrary, the specimens of mix R4 show the smallest peaks at 3400 cm^{-1} and 1000 cm^{-1}. Furthermore, at all of the spectra, the alumina and silicate bands increased as the curing times increases until mix R3, which contained 25% MCW and 5% HL. The band of amorphous silica at 800 cm^{-1} was observed and increased as the curing period increased, meaning that the smectite layer became substantially depleted.

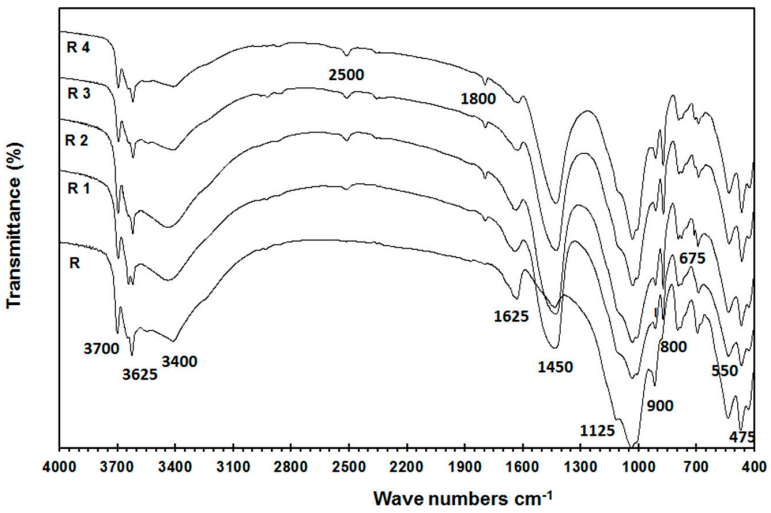

Figure 8. Fourier transformed infrared spectrometer (FTIR) spectra of the specimens of different mixes that were cured for two weeks.

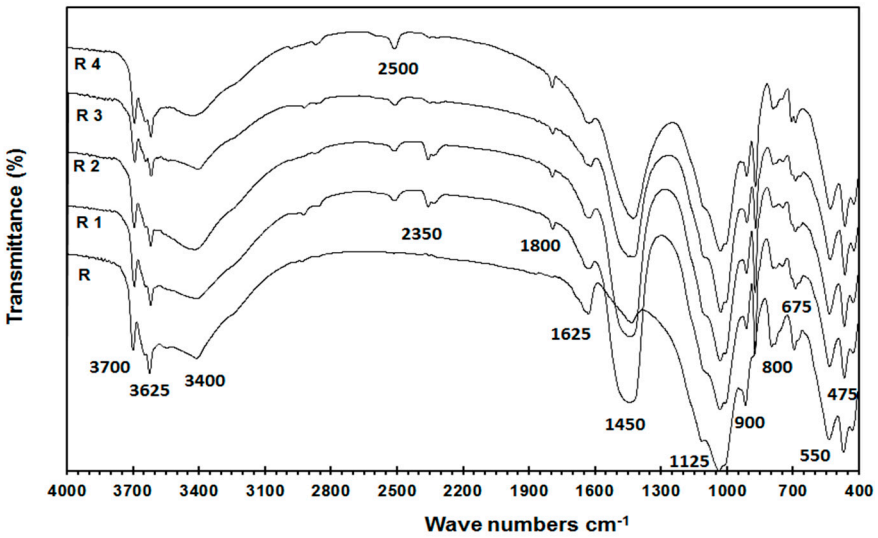

Figure 9. FTIR spectra of the specimens of different mixes that were cured for four weeks.

4. Conclusions

This research studied the feasibility of using marble cutting waste (MCW) with other additives for stabilizing clay–based materials to produce a sustainable, compressed, and stabilized clay brick. In the study, the materials used were characterized using different analytical tools and equipment; lab specimens made of five clay-based mixes were cured, dried, and tested. In summary, a potential benefit of stabilization was found to depend on the combination of hydrated lime and marble cutting waste. It was noticed the specimens of mix R could not be used successfully as a building unit without the stabilizers. Also, as the curing period proceeded and the MCW increased up to 15%, the water absorption and compressive strengths properties of the specimens improved. As shown in the XRD patterns and property results of the specimens of mix R4 without the HL, the gypsum and ettringite negatively affected the properties of the cured specimens. This study reveals that the MCW used worked well with a low content of HL (5%), as indicated by the specimen test results of mix R3, which has a pH value of 12.4. Furthermore, the specimens of mix R4 had the lowest physico-mechanical results, where the mix had no HL, and also possessed the lowest pH value, giving depressing impacts on the stabilization process. The applied silicon-based paint on the mixes and specimens enhanced the durability of the studied specimens against water, and this encourages its usage, especially in wet environments. The physico-mechanical test results of the specimens of mixes R1–R3 were located within the allowable requirements of the Egyptian code used (ECBS, 2016), as mentioned in Section 3.3. Finally, the using of MCW up to 15% in the studied mixes was feasible, and it is recommended to use mix R3 for the stabilized clay brick industry.

Author Contributions: Author M.S.E.-M. interpreted the data, wrote the manuscript and worked extensively on preparing the manuscript for publication. Author A.M.K. supervised and revised the work. Author M.L.A.L. conceived the research idea and participated in the practical work. Author A.M.E.N. participated in the practical experiments. All authors contributed to designing the study.

Acknowledgments: The authors gratefully acknowledge Ghada M. El-Mahdy of Structures and Metallic Construction Research Institute, Housing and Building National Research Center, Egypt for her help during reviewing the manuscript.

Conflicts of Interest: The authors declare no conflict of interest.

References and Notes

1. Reddy, B.; Jagadish, K. Embodied energy of common and alternative building materials and technology. *Energy Build.* **2003**, *35*, 129–137. [CrossRef]

2. Zhang, L. Production of bricks from waste materials—A review. *Constr. Build. Mater.* **2013**, *47*, 643–655. [CrossRef]
3. Turkmen, I.; Ekinci, E.; Kantarc, F.; Sarc, T. The mechanical and physical properties of unfired earth bricks stabilized with gypsum and Elazig Ferrochrome slag. *Int. J. Sus. Built Environ.* **2017**, *6*, 565–573. [CrossRef]
4. Siddiqua, S.; Barreto, P. Chemical stabilization of rammed earth using calcium carbide residue and fly ash. *Constr. Build. Mater.* **2018**, *169*, 364–371. [CrossRef]
5. Sekhar, D.; Nayak, S. Utilization of granulated blast furnace slag and cement in the manufacture of compressed stabilized earth blocks. *Constr. Build. Mater.* **2018**, *166*, 531–536. [CrossRef]
6. Sore, S.; Messan, A.; Prud'homme, E.; Escadeillas, G.; Tsobnang, F. Stabilization of compressed earth blocks (CEBs) by geopolymer binder based on local materials from Burkina Faso. *Constr. Build. Mater.* **2018**, *165*, 333–345. [CrossRef]
7. Rahman, M.; Rehman, S.; Al-Amoudi, O. Literature review on cement kiln dust usage in soil and waste stabilization and experimental investigation. *IJRRAS* **2011**, *1*, 77–87.
8. Zaliha, S.; Kamarudin, H.; Al Bakri, A.; Binhussain, M.; Salwa, M. Review on soil stabilization techniques. *Aust. J. Basic Appl. Sci.* **2013**, *7*, 258–265.
9. Galan-Marin, C.; Rivera-Gomez, C.; Petric, J. Clay-based composite stabilized with natural polymer and fiber. *Constr. Build. Mater.* **2010**, *24*, 1462–1468. [CrossRef]
10. Espuelas, S.; Omer, J.; Marcelino, S.; Echeverria, A.; Seco, A. Magnesium oxide as alternative binder for unfired clay bricks manufacturing. *Appl. Clay Sci.* **2017**, *146*, 23–26. [CrossRef]
11. Oti, J.; Kinuthia, J. Designed non-fired clay mixes for sustainable and low carbon use. *Appl. Clay Sci.* **2012**, *59*, 131–139.
12. Jawad, I.; Taha, M.; Majeed, Z.; Khan, T. Soil stabilization using lime: Advantages and proposing a potential alternative. *Res. J. Appl. Sci. Eng. Technol.* **2014**, *8*, 510–520.
13. Yesilay, S.; Munevver, C.; Ergun, H. Usage of marble wastes in traditional artistic stoneware clay body. *Ceram. Int.* **2017**, *43*, 8912–8921. [CrossRef]
14. Aliabdo, A.; Abd Elmoaty, A.; Auda, E. Re-use of waste marble dust in the production of cement and concrete. *Constr. Build. Mater.* **2014**, *50*, 28–41. [CrossRef]
15. Ghorbani, S.; Taji, I.; Tavakkolizade, M.; Davodi, A.; Brito, J. Improving corrosion resistance of steel rebars in concrete with marble and granite waste dust as partial cement replacement. *Constr. Build. Mater.* **2018**, *185*, 110–119. [CrossRef]
16. Bilgin, N.; Yeprem, H.; Arslan, S.; Bilgin, A.; Günay, A.; Marşoglu, A. Use of waste marble powder in brick industry. *Constr. Build. Mater.* **2018**, *29*, 449–457. [CrossRef]
17. Mashaly, A.; Shalaby, B.; El-Hefnawi, M. Characterization of the marble sludge of the Shaq El Thoban industrial zone, Egypt and its compatibility for various recycling applications. *Aust. J. Basic Appl. Sci.* **2012**, *6*, 153–161.
18. Zami, M.; Lee, A. Stabilized or unstabilized earth construction for contemporary urban housing. In Proceedings of the 5th International Conference on Responsive Manufacturing—Green Manufacturing, Ningbo, China, 11–13 January 2010.
19. El-Sayed, H.; Farag, A.; Kandeel, A.; Younes, A.; Yousef, M. Characteristics of the marble processing powder waste at Shaq El Thoban industrial zone, Egypt and its suitability for cement manufacture. *HBRC J.* **2016**, *14*, 171–179. [CrossRef]
20. Said, R. *The Geology of Egypt*, 3rd ed.; Elsevier Publ. Co.: Amesterdam, The Netherlands, 1962.
21. *ASTM DStandard Test Methods for Loss on Ignition (LOI) of Solid Combustion Residues*; Standard Annual Book of ASTM Standards; ASTM: West Conshohocken, PA, USA, 2008.
22. *ASTM D Standard Test Method for pH of Soils*; Standard Annual Book of ASTM Standards; ASTM: West Conshohocken, PA, USA, 2013.
23. Oti, J.; Kinuthia, J.; Bai, J. Engineering properties of unfired clay masonry bricks. *Eng. Geol.* **2009**, *107*, 130–139. [CrossRef]
24. Millogo, Y.; Hajjaji, M.; Ouedraogo, R. Microstructure and physical properties of lime-clayey adobe bricks. *Constr. Build. Mater.* **2008**, *22*, 2386–22392. [CrossRef]
25. Bahar, R.; Benazzoug, M.; Kenai, S. Performance of compacted cement-stabilised soil. *Cem. Concr. Compos.* **2004**, *26*, 811–820. [CrossRef]

26. Egyptian Code for the Building by the Soil (ECBS). The Building by the Stabilized and Compressed Earth Blocks; 2016; HBRC, Volume 1, pp. 1–144.
27. Egyptian Standard Specification (ESS). Quick and Hydrated Lime. Definitions, Requirements and Conformity Criteria; Egyptian Quality and Specification Association, Egypt, 2008.
28. El-Mahllawy, M. Effect of activation of granulated blast-furnace slag on the properties of unfired eco-friendly clay bricks. In Proceedings of the 1st International Conference on Innovative Building Materials, Cairo, Egypt, 28–30 December 2014.
29. El-Mahllawy, M.; Kandeel, A. Engineering and mineralogical characteristics of stabilized unfired montmorillonitic clay bricks. *HBRC J.* **2014**, *10*, 82–91. [CrossRef]
30. Nair, S.; Little, D. Mechanisms of distress associated with sulfate-induced heaving in lime-treated soils. *Transp. Res. Record J. Trans. Res. Board* **2011**, *2212*, 82–90. [CrossRef]
31. Abd Elaty, M.; Ghazy, M. Performance of Portland cement mixes containing silica fume and mixed with lime-water. *HBRC J.* **2014**, *10*, 247–257. [CrossRef]
32. Choller, M.; Horgnies, M. Analyses of the surface of concrete by Raman and FT-IR spectroscopies comparative study of hardened samples after demoulding and after organic post-treatment. *Surf. Interface Anal.* **2010**, *43*, 714–725. [CrossRef]
33. Djomgoue, P.; Njopwouo, D. FT-IR spectroscopy applied for surface clays characterization. *J. Surf. Eng. Mat. Adv. Technol.* **2013**, *3*, 275–282. [CrossRef]
34. Madejova, J. FTIR techniques in clay minerals studies. *Vib. Spectrosc.* **2003**, *31*, 1–10. [CrossRef]
35. Yu, P.; Kirkpatrick, R.; Poe, B.; McMillan, P.; Cong, X. Structure of calcium silicate hydrate (C-S-H): Near-, mild-, and far-infrared spectroscopy. *J. Am. Ceram. Soc.* **1999**, *82*, 742–748. [CrossRef]